Available at www.sciencedirect.com

ScienceDirect

journal homepage: www.elsevier.com/locate/he

Investigation of metal alloy catalyst for hydrogen release from sodium borohydride for polymer electrolyte membrane fuel cell application

Joon-Hyun Park[a], *Piraman Shakkthivel*[a], *Hyun-Jong Kim*[b], *Myung-Keun Han*[b], *Jae-Hyuk Jang*[c], *Yong-Rok Kim*[d], *Han-Sung Kim*[a], *Yong-Gun Shul*[a,*]

[a]*Department of Chemical Engineering, Yonsei University, 134 Shinchon-dong, Seodaemun-Gu, Seoul 120-749, Republic of Korea*
[b]*Nano Surface Technology, Korea Institute of Industrial Technology, 7-47 Songdo-dong, Yeonsu-Gu, Incheon, Republic of Korea*
[c]*Corporate R&D Center, Samsung Electro-Mechanics, 314 Maetan-Dong, Yeongtong-Gu, Suwon, Gyunngi-Do 443-743, Republic of Korea*
[d]*Department of Chemistry, Yonsei University, 134 Shinchon-dong, Seodaemun-Gu, Seoul 120-749, Republic of Korea*

ARTICLE INFO

Article history:
Received 17 October 2007
Received in revised form
19 December 2007
Accepted 7 January 2008
Available online 17 March 2008

Keywords:
Sodium borohydride
Combinatorial
Hydrogen release
Alloy catalyst

ABSTRACT

Sodium borohydride ($NaBH_4$) is a promising candidate for storing hydrogen in portable fuel cell systems. In order to reduce the volume and cost of the hydrogen generation systems, a high-performance catalyst containing a less precious metal is imperative. In this present investigation, a number of metal alloy compositions are compared in a high throughput screening (HTS) test. In the case of tertiary alloy suspension, the hydrogen release rate of $Ru_{60}Co_{20}Fe_{20}$ shows highest H_2 release (26.8 L min^{-1} g^{-1}). In the case of the activated carbon fiber (ACF) supported ruthenium catalyst, the reduction process plays an important role in both the particle size of the formed catalyst and consequent enhancement of the hydrogen release rate. $Ru_{60}Co_{20}Fe_{20}$/ACF showed its highest hydrogen release rate at 41.73 L min^{-1} g_{Ru}^{-1}. The prepared catalysts were analyzed by XRD and XPS spectra. The suitability of the catalyst in the real proton exchange membrane fuel cell application has been examined and it shows the applicability for common use.

1. Introduction

Hydrogen has been recognized as the premier energy carrier for the future energy system. The development of hydrogen-based energy economy with the use of sustainable energy sources promises to alleviate numerous current problems such as air pollution, greenhouse gas production, and global security [1]. Hydrogen is a clean synthetic fuel, which when burnt with oxygen, emits water vapor as its sole byproduct [2]. Fuel cells are an alternative energy system utilizing hydrogen gas in the production of energy. In the polymer electrolyte membrane fuel cell (PEMFC) systems, hydrogen and oxygen are converted by an electrochemical reaction and produce electric energy without any combustion [3].

In order to realize the fuel cell systems for the mobile and portable applications, the hydrogen storage and distribution system must be of economical size and weight, particularly for the transportation sector. Currently, there are many hydrogen storage materials such as pressurized hydrogen, liquefied hydrogen, physico-chemical adsorption, metal hydride, and chemical hydride [1,2].

Nowadays, much attention has been given to the hydrolysis of chemical hydrides, especially sodium borohydride because of its high gravimetric (up to hydrogen density of 10.9 wt%)

*Corresponding author. Tel.: +82 2 2123 2758; fax: +82 2 312 6401.
E-mail address: shulyg@yonsei.ac.kr (Y.-G. Shul).
0360-3199/$ - see front matter © 2008 International Association for Hydrogen Energy. Published by Elsevier Ltd. All rights reserved.
doi:10.1016/j.ijhydene.2008.01.003

and volumetric densities [4,5]. Moreover, sodium borohydride is non-flammable and non-toxic, easily liberates hydrogen with low temperature, and its spent fuel (sodium metaborate) is environmentally friendly [6].

Sodium borohydride generates four moles of hydrogen and one mole of sodium metaborate when one mole of sodium borohydride reacts with two moles of water [7] as shown in the following equation:

$$NaBH_4 + 2H_2O \rightarrow NaBO_2 + 4H_2 + Q. \quad (1)$$

(The exothermic reaction releases approximately 55 kJ of heat per mole of hydrogen.)

Decomposition of sodium borohydride occurring in aqueous media is negligible without the acceleration by the catalyst. The decomposition rate of sodium borohydride is dependent on the temperature and pH [7]. Therefore, basic (pH > 13) solutions of aqueous borohydride are used for hydrogen storage in order to inhibit the release of the hydrogen from sodium borohydride solution in the absence of a borohydride hydrolysis catalyst. Hydrogen generation by hydrolysis of borohydride dissolved in aqueous alkaline solution can be accelerated by metal catalysts [6–24], acids [5,25], and elevated temperatures [26,27]. In the case of acid-accelerated hydrogen release, the rate depends on the pH, the species of the acid, and the salts used in the buffer. Acidic accelerators are consumed after the hydrolysis reaction [25].

There has been much research performed on the hydrogen release using catalysts. Several metal catalysts are effective reaction catalyst for the enhancement of hydrolysis, among them: raney nickel [7], nickel or cobalt borides [8–11], cobalt on γ-alumina [12], Co–P catalyst [13], ruthenium nanoparticle [14], ruthenium supported on IRA-400 resin [6,15] or alumina pellet [16], platinum supported on $LiCoO_2$ [17–19] or carbon [20], metal nanocluster [21–23], and Pt/Pd on carbon nanotube (CNT) paper [24]. However, there is no report employing the alloy catalyst to enhance the hydrolysis reaction of the alkaline sodium borohydride solution. But, wide ratios of metal alloys are not yet tested to increase the hydrogen release rate at room temperature. In our present study, a number of different binary and ternary alloys have been synthesized and their catalytic effect on the hydrogen release from the alkaline sodium borohydride solution was examined by using combinatorial technique. The effect of activated carbon support for the catalyst on the hydrogen release and the PEMFC-integrated hydrogen production were also investigated in order to develop a high performance catalyst for hydrogen generation.

2. Experimental

2.1. Materials and methods

Ruthenium(III) chloride ($RuCl_3 \cdot 3H_2O$, Kojima Chemical Co.), iron(II) chloride ($FeCl_2 \cdot 4H_2O$, Wako Pure Chemical Co.), cobalt nitrate ($Co(NO_3)_2 \cdot 6H_2O$, Junsei Chemical Co.), nickel(II) chloride ($NiCl_2 \cdot 6H_2O$, Sigma-Aldrich), palladium(II) chloride ($PdCl_2$, Kojima Chemical Co.), silver nitrate ($AgNO_3$, Kojima Chemical Co.), and copper(II) chloride ($CuCl_2 \cdot 2H_2O$, Aldrich Chemical Co.) were purchased and used as received. All the required solutions and precursor samples were prepared using de-ionized water. Concentration of the salts was adjusted to 25 $g_{metal}\,L^{-1}$. According to the weight ratio of metals, each micro-reactor contains 100 μL (equal to 2.5 mg metal) of mixed precursor. After sealing the micro-reactor, 10 ml of 10 wt% of sodium borohydride +4 wt% of sodium hydroxide solution was added to each micro-reactor. A reduction time of 30 min was allowed for complete reduction of the Ru, Fe, and Co salts. After 30 min, hydrogen released from the reactors was collected, and the cumulative amount of hydrogen was gathered in the glass syringe. It was also evaluated by GFC mass controller (Aalborg Co.).

2.2. Catalyst screening by HTS test

Sodium borohydride is not only useful for hydrogen storage but also an excellent reducing agent. It reacts with various metal salts and is able to reduce the metal salts into the metal even in suspension. When $H_2PtCl_6 \cdot 6H_2O$ and $RuCl_3 \cdot 3H_2O$ are reduced by sodium borohydride, platinum and ruthenium black are formed, respectively [14]. It is easy to form the metal alloy suspension by co-reducing more than two metal salts. The main focus was on the metal alloy suspension due to its high catalytic activity toward the hydrolysis reaction of sodium borohydride solution. Since the hydrolysis reaction can occur after the reduction process in the sodium borohydride solution, the reduction and hydrolysis reaction were simplified in a single-step-experiment to observe the catalytic activity of metal alloy suspensions on hydrogen release from the sodium borohydride solution. As shown in Fig. 1, evaluation of the catalytic activity of the metal alloy suspension can be carried out by adding sodium borohydride solution into the micro-reactor that contains mixed precursor solution. A number of micro-reactors were filled with the mixed precursor solution and sealed. Micro-reactors were fixed in the high throughput screening (HTS) test reactor as shown in Fig. 2. Each glass syringe and gas vent line was connected to each micro-reactor. The hydrolysis reaction of sodium borohydride is exothermic, hence the temperature of the HTS test reactor was maintained by circulating cold water.

2.3. Preparation of catalyst on carbon support

Two different source of carbon, ACF, with a specific surface area of 1500 m^2/g purchased by Kuraray Chemical Co. and Vulcan XC-72R were used as the support for the metallic

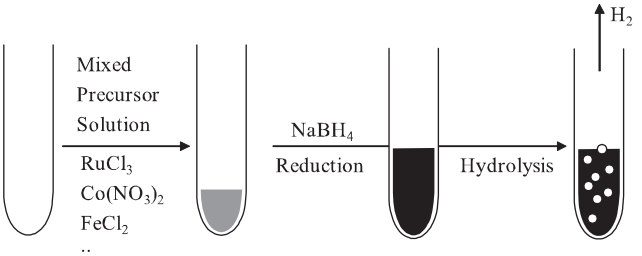

Fig. 1 – The reduction and hydrolysis reaction between metal salts and sodium borohydride solution.

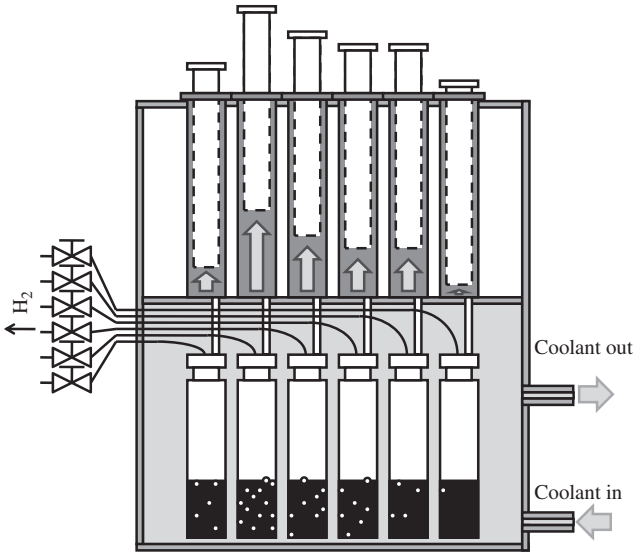

Fig. 2 – HTS test reactor.

catalysts. Ru/C (or ACF) catalyst was prepared by different methods. Initially, a 0.2 M ruthenium chloride solution was prepared by dissolving 0.259 g of $RuCl_3 \cdot 3H_2O$ in 5 ml of deionized water and 10:90% of Ru:C (or ACF) was prepared by the addition of required carbon into the $RuCl_3 \cdot 3H_2O$ solution. The above solution was stirred for 3 h and sonicating for 30 min and then allowed to dry. The synthesized catalyst was dried in an oven at 80 °C and the reduction of ruthenium chloride was performed using three different methods. In the first method, it was reduced using sodium borohydride, and in the second, $RuCl_3 \cdot 3H_2O$ was reduced in the hydrogen atmosphere at 400 °C for 6 h. In the final method, metallic halide was reduced using a combination of the first two methods. Similar method has been adopted for the preparation of RuCo/ACF and RuCoFe/ACF catalysts. The influence of temperature on the catalytic activity of synthesized catalyst in the hydrogen release from the sodium borohydride solution has been examined in the temperature range of 15–35 °C with a step value of 5 °C.

2.4. *Characterization*

The formation of metals reduced from the metallic halides was examined through the X-ray diffraction (XRD) studies. XRD patterns were obtained using a Rigaku Miniplex system operating at 30 kV and 15 mA. X-ray photoelectron spectra (XPS) measurements were also performed on an EscaLab 220-IXL system with an aluminum filament, using the Kα line. The binding energies were calibrated using the C–C 1 s photoelectron peak at 284.8 eV. The Co 2p, Fe 2p, and Ru 3p lines were obtained to observe the alloy formation.

3. Results and discussion

3.1. *Suspension catalysts screening by HTS test*

Ruthenium was chosen as a primary metal and cobalt, nickel, and iron were used as secondary metals with different weight ratios. The hydrogen release rates of the binary suspension catalysts are shown in Fig. 3. Cobalt reduced with sodium borohydride showed high catalytic activity [8–11], equal only to that of ruthenium. Iron showed poor activity when employed for monometallic suspension, but its activity increased dramatically when a small amount of iron was added to the ruthenium. $Ru_{80}Fe_{20}$ suspension exhibited the highest activity of 18.3 L min^{-1} g^{-1}, which is around 275% higher than the Ru/Co alone. At higher concentrations of iron in ruthenium, the catalytic activity is reduced to zero. The addition of cobalt in the ruthenium around 40–80%, offers constant H_2 release with a 250% enhancement in their catalytic activity when compared with their mono catalyst. Nickel also showed positive results in binary alloy system, even small improvement. In case of palladium, silver, and copper, however, hydrogen release rate was only dependent on the amount of ruthenium.

For the optimization of percentage of metals in their composition, 36 different composition (Ru–Co–Ni, Ru–Co–Fe) have been examined for their catalytic activity toward the release of H_2 from sodium borohydride solution and the results are depicted in Fig. 4. There is only very little alloy effect in Ru–Ni for the hydrogen release. However, the addition of (20%) cobalt in the Ru–Ni, higher catalytic activity was recorded. In the case of tertiary alloy suspension, the hydrogen release rate is higher in the Ru–Co–Ni alloy, but its catalytic activity is very small (less than a half) when compared with the binary metal alloy composition (Ru–Co or Ru–Fe at $Ru_{80}Co_{20}$/$Ru_{80}Fe_{20}$). From Fig. 4(a), it can be inferred that the addition of nickel in the Ru–Co alloy does not show any synergistic effect on the hydrogen generation from sodium borohydride. Fig. 4(b) depicts the catalytic activity of Ru–Co–Fe on the hydrolysis of sodium borohydride. The addition of Co/Fe in the ruthenium suspension from 0% to 100%, there is an increase in hydrogen release from ~6 to ~16 L min^{-1} g^{-1} up to 40–80% and 20% addition of Co and Fe, respectively. Beyond 20%, the trend is decline to 0 L min^{-1} g^{-1} at 100% Fe. However, with the addition of 20% Fe and 20% Co

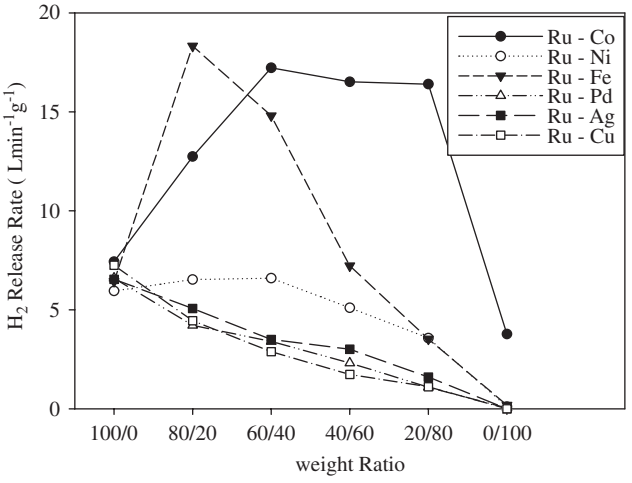

Fig. 3 – Hydrogen release rate of binary metal suspensions in 10 wt% sodium borohydride with 4 wt% sodium hydroxide solution at 25 °C.

to the Ru suspension catalyst, the hydrogen generation progressively increased to 26.8 L min^{-1} g^{-1}. This may be due to the addition of Fe, which acts as an alloy with Ru and Co and reduces the catalytic degradation with enhanced performance. The sharp increase in the catalytic activity of Co/Fe in Ru–Fe/Ru–Co is observed.

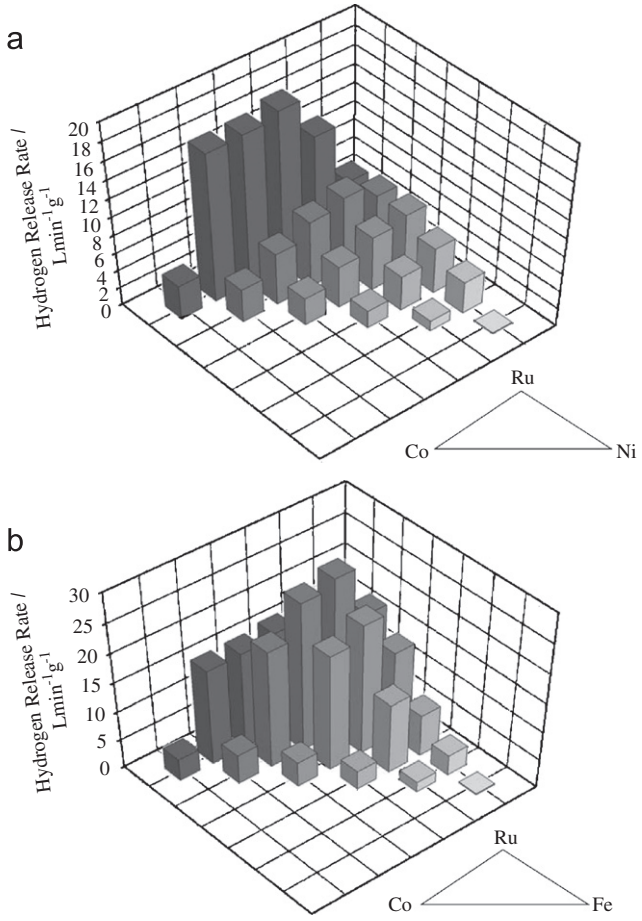

Fig. 4 – Hydrogen release rate of ternary metal suspensions in 10 wt% sodium borohydride with 4 wt% sodium hydroxide solution at 25 °C: (a) Ru–Co–Ni and (b) Ru–Co–Fe.

3.2. *ACF support*

In the HTS test with suspension catalysts, there was no remarkable decline of hydrogen release rate in the first hour. However, beyond 60 min, the rate of hydrogen release decreased gradually with macroscopic changes of coagulating metal suspension. In order to prevent the agglomeration of the metal suspension and improve the hydrogen release rate, supporting materials such as IRA-400 resin [6,15], $LiCoO_2$ [17–19], and Vulcan C [28] were employed in the previous investigations. In our present study, ACF and Vulcan C were used as supporting materials to prepare a highly dispersed metal alloy catalyst. A 10% Ru/C (or ACF) was prepared using the reduction method with hydrogen, sodium borohydride, and both as described in Section 2. The efficiency of catalysts in releasing hydrogen from sodium borohydride prepared by different reduction methods are listed in Table 1. Ruthenium supported by Vulcan XC-72R reduced with hydrogen and sodium borohydride, the hydrogen reduced Ru/C show 50% higher catalytic activity. In the case of the ACF supported ruthenium catalyst, the reduction process plays an important

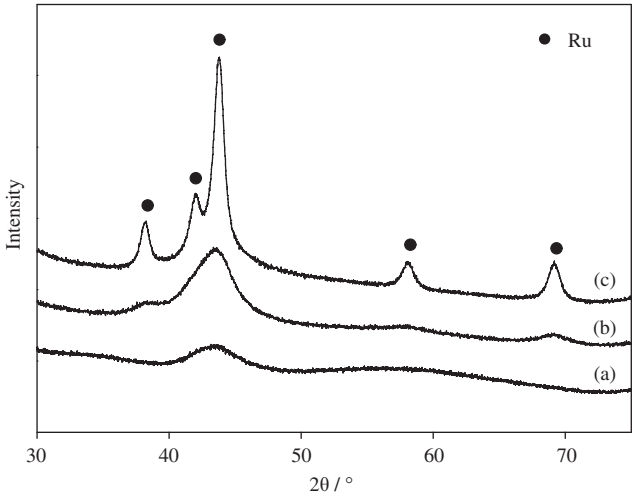

Fig. 5 – XRD patterns of the samples: (a) RAH, (b) RAN, and (c) RANH.

Table 1 – Ruthenium catalyst on the support materials

Catalyst	Composition	Reduction agent	Hydrogen release rate (L min^{-1} g_{Ru}^{-1})	Calculated particle size (nm)	Reference
RCH	10% Ru/C	H_2	9.83	–	
RCN	10% Ru/C	$NaBH_4$	6.97	–	
RAH	10% Ru/ACF	H_2	13.62	2.15	
RAN	10% Ru/ACF	$NaBH_4$	5.50	4.58	
RANH	10% Ru/ACF	$NaBH_4 + H_2$	4.90	9.21	
Ru/IRA-400	5% Ru/IRA-400	$NaBH_4$	5.10	–	[6]
$Ru/LiCoO_2$	10% $Ru/LiCoO_2$	$NaBH_4$	10.24	–	[18]

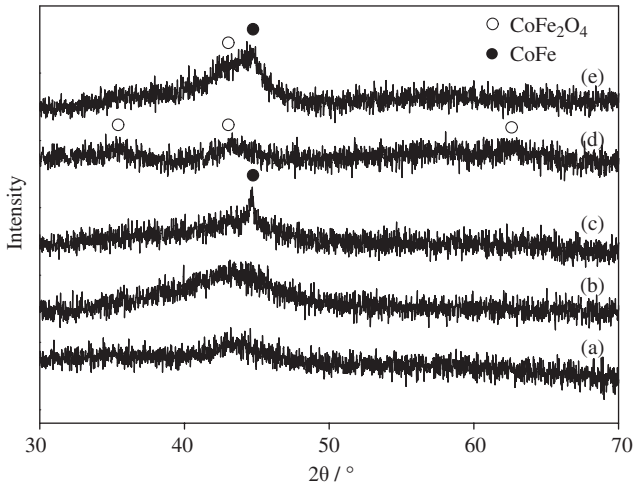

Fig. 6 – XRD patterns of the samples: (a) RC–N, (b) RC–NH, (c) RCF–H, (d) RCF–N, and (e) RCF–NH.

role in both the particle size of the formed catalyst and consequent enhancement of the hydrogen release rate.

3.3. *Characterization*

According to the previous studies [19,24], it is reported that the catalytic activity of the platinum catalyst toward the hydrolysis reaction of sodium borohydride solution is dependent on the size of platinum particles. In order to find out the association of the catalytic activity with the particle size of the ruthenium catalyst, XRD analysis was carried out. The XRD patterns of the 10% Ru/ACF catalysts prepared by different reduction methods are presented in Fig. 5. Particle size of the Ru (1 0 1) was calculated by means of Scherrer's equation, as shown in the following equation:

$$D(\text{Å}) = k\lambda/\beta\cos\theta. \quad (2)$$

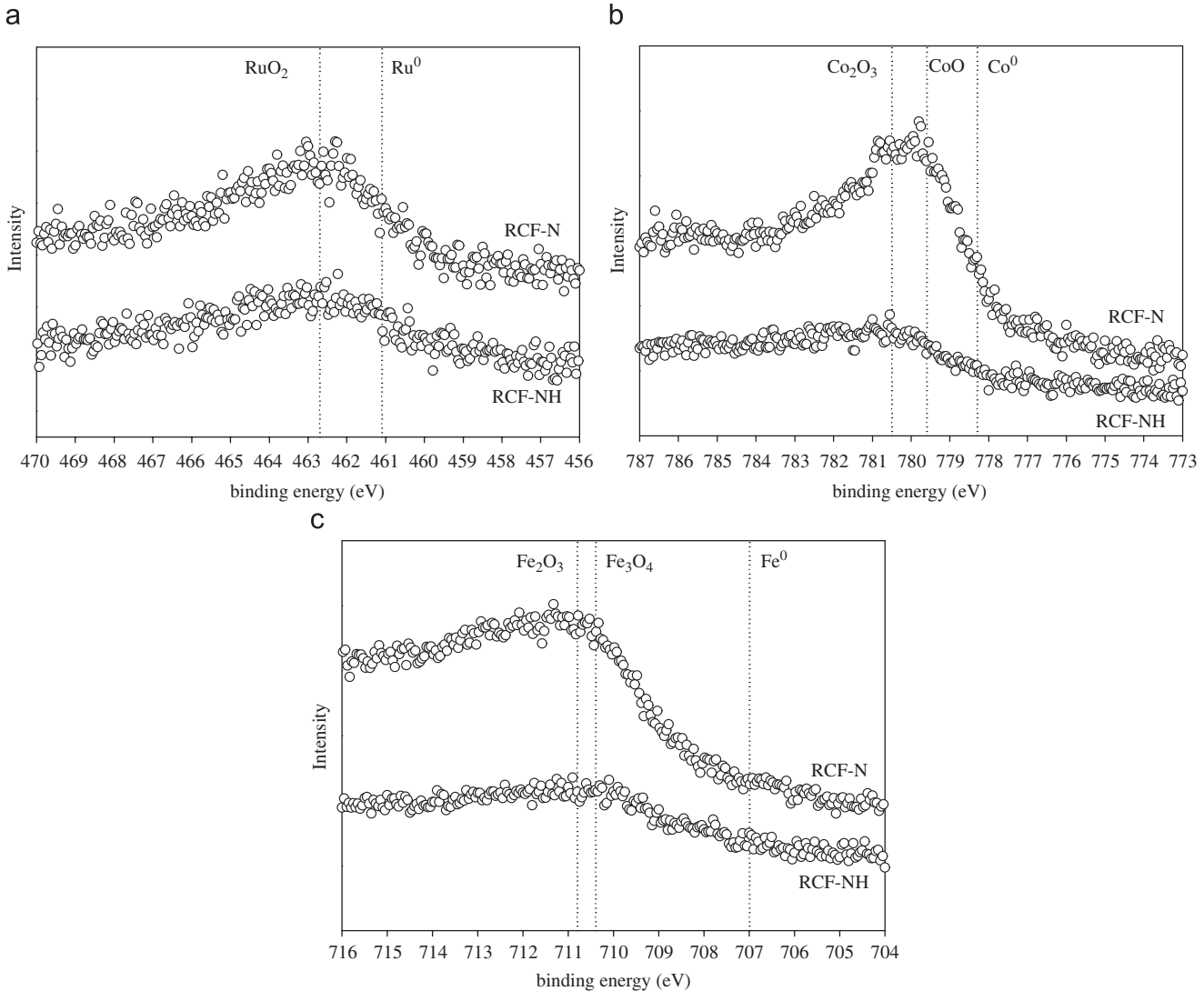

Fig. 7 – XPS of RCF–N and RCF–NH in: (a) Ru $3p_{3/2}$, (b) Co $2p_{3/2}$, and (c) Fe $2p_{3/2}$.

The presence of the ruthenium in the ACF supported catalyst is confirmed in all the patterns. All the catalysts prepared are abbreviated (e.g. RAH is ruthenium/ACF reduced by hydrogen) in Table 1. RAH is observed to be an amorphous form, thus it is implied that ruthenium is well dispersed on the surface of the ACF. The calculated particle size of the ruthenium is 2.15 nm, however, in the case of RANH (ruthenium/ACF reduced by $NaBH_4$ and then H_2), the crystalline structure of the material increased tremendously with a particle size (9.21 nm), which is much larger than that of RAN (ruthenium/ACF reduced by $NaBH_4$) (4.58 nm) or RAH (2.15 nm). The smaller particle size with a higher active surface area enormously helps to produce enhanced progressive hydrogen release from the sodium borohydride.

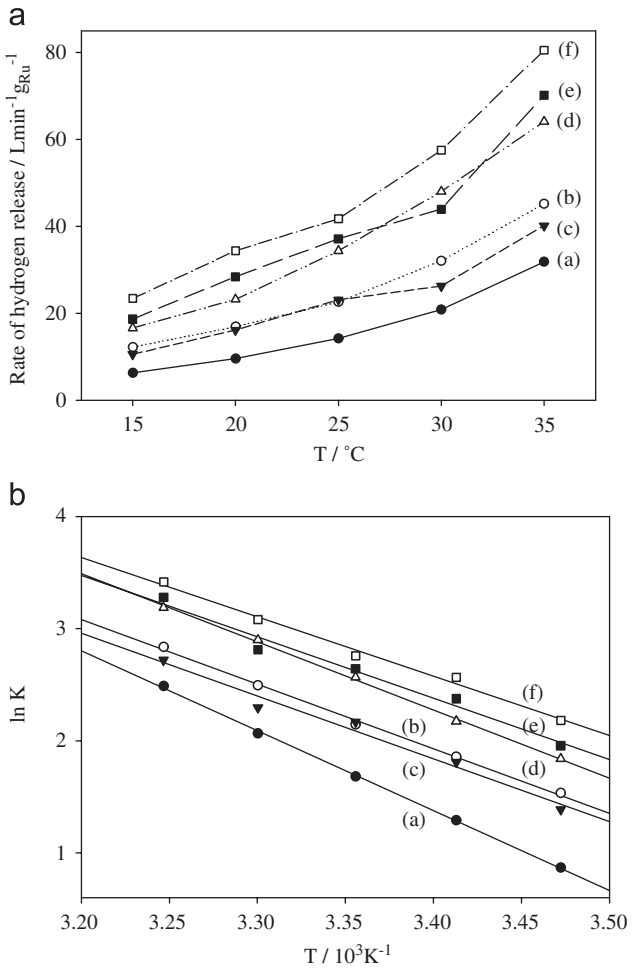

Fig. 8 – Catalytic activity of the catalysts: (a) RAH, (b) RCF–H, (c) RC–N, (d) RCF–N, (e) RC–NH, and (f) RCF–NH presented by (A) hydrogen release rate and (B) Arrhenius plot.

The XRD spectra of ruthenium–metal alloys are shown in Fig. 6. In all the XRD patterns, the peak for ruthenium is not clear. Ru–Co/ACF catalysts (Figs. 6(a) and (b)) showed an amorphous form, and thus it is hard to verify the broad peak around 44° whether it indicates Ru, Co, or the Ru–Co alloy. The sharpest peaks for Co and Co_2B appears at 44.3° and 45.7°, respectively [29], but the nearest peak of Co_2B departs from the main peak of Fig. 4(a), so it is not detected. Even after the hydrogen reduction of RC–N, the intensity of the main peak near 44° is increased, but the amorphous phase is not extinct (Fig. 6(b)). In Fig. 6(c), a sharp peak observed at around 44° is assigned for the Co–Fe alloy and it can be inferred that the cobalt and iron particles were sintered during the reduction. When the cobalt and iron were co-reduced with sodium borohydride (Fig. 6(d)), only weak $CoFe_2O_4$ spinel peaks are observed in the XRD pattern. Though the molecular ratio of the cobalt and iron precursors was 1:1, no $CoFe_2O_4$ spinel peak is detected in XRD analysis. Thus, it is suggested that the Ru–Co alloy was partially formed with the $FeCo_2O_4$ spinel during the reduction process. After the additional reduction, which catalyst denoted as RCF–NH, $CoFe_2O_4$ spinel peaks almost disappeared and a clear Co–Fe peak was found.

The surface composition and chemical states of the prepared catalysts were examined by XPS analysis. Fig. 7 shows the XPS spectra of RCF–N and RCF–NH. As the Ru 3d line is very close to the C 1 s line due to the ACF, the Ru $3p_{3/2}$ region is observed. The binding energy (BE) of the Ru $3p_{3/2}$ peak is 461.1 and 462.7 eV, which correspond to Ru^0 and Ru^{4+}, respectively [30]. The Ru^{4+} peak is mainly observed in both of the RCF–N and RCF–NH. It indicates that the surface of Ru was completely modified with Co and Fe, thus the presence of oxidized ruthenium content is much higher than that of the metallic ruthenium. In the photoelectron spectra of Co $2p_{3/2}$

Table 2 – Catalytic activity of alloy catalysts

Catalyst	Composition	Reducing agent	Hydrogen release rate at 25 °C (L min^{-1} g$_{Ru}^{-1}$)	Activation energy (kJ mol^{-1})
RAH	10% Ru/ACF	H_2	14.21	59.23
RCF–H	16.6% $Ru_{60}Co_{20}Fe_{20}$/ACF	H_2	22.63	47.91
RC–N	13.3% $Ru_{75}Co_{25}$/ACF	$NaBH_4$	23.11	46.57
RCF–N	16.6% $Ru_{60}Co_{20}Fe_{20}$/ACF	$NaBH_4$	34.37	50.54
RC–NH	13.3% $Ru_{75}Co_{25}$/ACF	$NaBH_4 + H_2$	37.12	45.44
RCF–NH	16.6% $Ru_{60}Co_{20}Fe_{20}$/ACF	$NaBH_4 + H_2$	41.73	44.01

line, Co^{3+} and Co^{2+} are present at the main peak while Co^0 was not detected. The BE of the Co $2p_{3/2}$ peaks are 780.5, 779.6, 778.4, and 778.3 eV, which are attributed to Co^{3+}, Co^{2+}, Co_2B, and Co^0, respectively [31–33]. The Co^{2+} peak is only 0.1 eV higher than the BE of the $CoFe_2O_4$ spinel peak (779.7 eV) [34]. It indicates the presence of $CoFe_2O_4$ in RCF–N. In the Fe $2p_{3/2}$ photoelectron line, two oxidation states and Auger feature of the Co $L_3M_{45}M_{45}$ (BE = 713 eV) [35] are found. There was some difficulty quantitatively analyzing the preferred oxidation states between Fe_2O_3 and Fe_3O_4. However, it is clearly evident that the Fe^0 peak is detected as just a small fraction of the Fe $2p_{3/2}$ line. The BE of the Fe $2p_{3/2}$ peaks are 710.8, 710.4, and 707.0 eV, which are assigned for Fe_2O_3, Fe_3O_4, and Fe^0, respectively [35]. The oxidized status of Ru, Co, and Fe was found through the XPS studies in the alloy catalyst.

3.4. *Hydrogen release test of catalyst*

Prepared catalysts were examined by the HTS test reactor. Ru–Co/ACF catalysts exhibit much higher performance than the Ru/ACF catalyst as shown in Fig. 8. Though the XRD analysis showed only a slight difference in intensity, with an amorphous peak near 44° between the Ru–Co/ACF alloy catalysts, the catalytic activity is significantly different. The hydrogen release rate of the Ru–Co–Fe/ACF catalysts (Figs. 8(e) and (f)) was higher than that of the Ru–Co/ACF catalysts (Figs. 8(b) and (c)). It is clear that addition of Fe induced the enhancement of catalytic activity of the Ru–Co/ACF while the reducing agent was sodium borohydride, which was same result as the HTS test. However, there was only a minimal improvement by the addition of Fe when a further hydrogen reduction process was employed. Therefore, it is concluded that the Ru–Co or Co–Fe alloys are preferred to the Ru–Fe alloy. Moreover, Fe tends to be present in an oxidized form as occurs in a $CoFe_2O_4$ spinel. Iron may cover the surface of ruthenium and thus the activity is decreased. An attempt to synthesize a Ru–Fe alloy was unsuccessful.

For the comparison of previous studies, the activation energy was calculated by the temperature change in hydrogen release rate of the catalyst and these changes were recorded. The activation energy can be arrived at using the Arrhenius equation:

$$k = A\exp(-E_a/RT). \quad (3)$$

As shown in Table 2, activation energy of RCF–NH is 44.01 kJ mol^{-1}, which is much lower than that of pristine ruthenium (59.23 and 56.13 kJ mol^{-1} for RAF and Ref. [6], respectively).

3.5. *PEMFC-integrated hydrogen generation system*

A catalyst-accelerated hydrogen generation system was developed and integrated with the PEMFC system. Sodium borohydride or pressurized hydrogen was employed as a hydrogen source and shown in Fig. 9. A hydrogen generation system was loaded utilizing an aqueous sodium borohydride solution

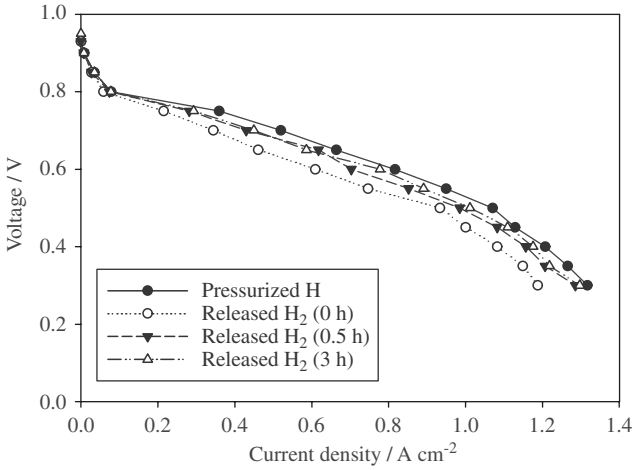

Fig. 10 – I–V curve of PEMFC cell.

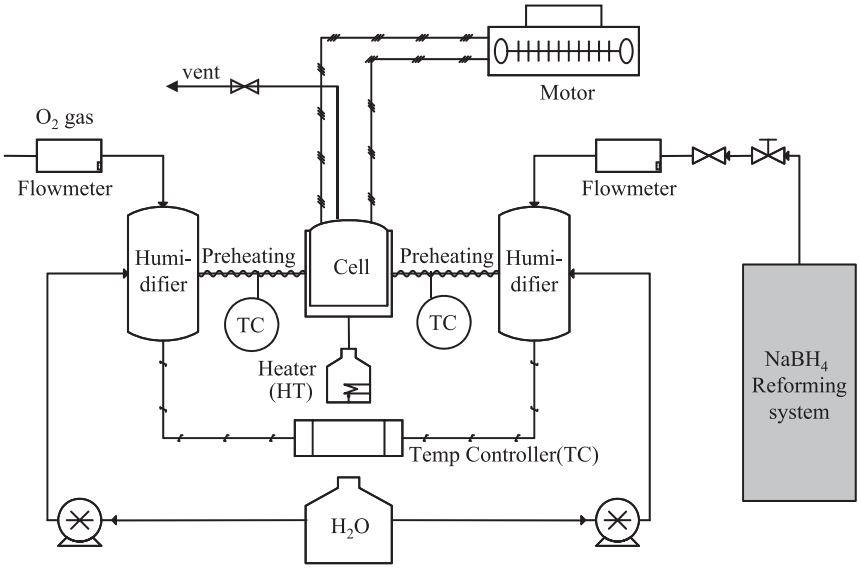

Fig. 9 – The PEMFC system using sodium borohydride solution as hydrogen source.

containing 10 wt% sodium borohydride and 4 wt% sodium hydroxide. The solution was stirred and the temperature was fixed to 30 °C. Catalyst RCF–NH was employed as an accelerator for generating hydrogen from the sodium borohydride solution. At first, the PEMFC cell was activated with pressurized hydrogen for the first 48 h and then an *I*–*V* curve was obtained, as shown in Fig. 10. When the hydrogen source was converted to a sodium borohydride solution, the performance of the cell was initially diminished by over 20%, but, after 3 h, its aptitude gradually increased and almost equaled the performance of pressurized hydrogen.

4. Conclusion

The catalyst screening for the accelerated hydrolysis of sodium borohydride was accomplished. The HTS test system was developed and employed to investigate alloy catalyst consisted of transition metals such as ruthenium, cobalt, iron, and nickel. A 20% addition of Fe in Ru binary alloy shows the highest activity (18.3 L min^{-1} g^{-1}). However, the addition of Co in Ru exhibits the activity of 17.2 L min^{-1} g^{-1}. Among the tested alloy suspension catalyst, $Ru_{60}Co_{20}Fe_{20}$ offers highest catalytic activity on the sodium borohydride hydrolysis. The composition of the $Ru_{60}Co_{20}Fe_{20}$, was prepared with ACF support by different reduction methods. The synthesized alloys structures were examined through the XRD and XPS studies and confirmed the formation of the Ru–Co–Fe alloy. The performance of the catalyst was examined for common use, and the results show that it has the potential to allow for the construction of a more space-efficient PEMFC.

Acknowledgments

This work is supported by the International Joint Research Program of KOCI (Korea Research Council for Industrial Science and Technology), the fostering project of the Specialized Graduate School of Hydrogen and Fuel Cell and New and Renewable Energy R&D program (2005-N-FC12-P-02) supported financially by the Ministry of Commerce, Industry, and Energy (MOCIE) and the Nano R&D program funded by the Ministry of Science and Technology, Republic of Korea (M1-0203-00-0003).

REFERENCES

[1] Zhang J, Fisher TS, Gore JP. J Heat Transfer 2005;127:1391–9.
[2] Schlapbach L, Züttel A. Nature 2001;414:353–8.
[3] Jang W, Sundar S, Choi S, Shul YG, Han H. J Membr Sci 2006;280(1+2):321–9.
[4] Han MK, Han JH, An K, Jeon DS, Gervasio D, Song I, et al. Mater Sci Forum 2007;539–543:2295–300.
[5] Kojima Y, Kawai Y, Nakanishi H, Matsumoto S. J Power Sources 2004;135:36–41.
[6] Amendola SC, Sharp-Goldman SL, Janjua MS, Spencer NC, Kelly MT, Petillo PJ, et al. Int J Hydrogen Energy 2000;25:969–75.
[7] Schlesinger HI, Brown HC, Finholt AE, Gilbreath JR, Hoekstra HR, Hyde EK. J Am Chem Soc 1953;75:215–9.
[8] Levy A, Brown JB, Lyons CJ. Ind Eng Chem 1960;52:211–4.
[9] Kaufman CM, Sen B. J Chem Soc Dalton Trans 1985;2:307–13.
[10] Lee J, Kong KY, Jung CR, Cho E, Yoon SP, Han J, et al. Catal. Today 2007;120:305–10.
[11] Jeong SU, Cho EA, Nam SW, Oh IH, Jung UH, Kim SH. Int J Hydrogen Energy 2007;32:1749–54.
[12] Ye W, Zhang H, Xu D, Ma L, Yi B. J Power Sources 2007;164:544–8.
[13] Cho KW, Kwon HS. Catal Today 2007;120:298–304.
[14] Brown HC, Brown CA. J Am Chem Soc 1962;84:1493–4.
[15] Amendola SC, Sharp-Goldman SL, Janjua MS, Kelly MT, Petillo PJ, Binder M. J Power Sources 2000;85:186–9.
[16] Zhang JS, Delgass WN, Fisher TS, Gore JP. J Power Sources 2007;164:772–81.
[17] Kojima Y, Suzuki K, Fukumoto K, Kawai Y, Kimbara M, Nakanishi H, et al. J Power Sources 2004;125:22–6.
[18] Krishnan P, Yang TH, Lee WY, Kim CS. J Power Sources 2005;143:17–23.
[19] Kojima Y, Suzuki K, Fukumoto K, Sasaki M, Yamamoto T, Yawai Y, et al. Int J Hydrogen Energy 2002;27:1029–34.
[20] Xu D, Zhang H, Ye W. Catal Commun 2007;8:1767–71.
[21] Özkar S, Zahmakıran M. J Alloys Compd 2005;404–406:728–31.
[22] Zahmakıran M, Özkar S. J Mol Catal A Chem 2006;258:95–103.
[23] Metin Ö, Özkar S. Int J Hydrogen Energy 2007;32:1707–15.
[24] Peña-Alonso R, Sicurelli A, Callone E, Carturan G, Raj R. J Power Sources 2007;165:315–23.
[25] James BD, Wallbridge MGH. Prog Inorg Chem 1970;11:99–231.
[26] Aicllo R, Sharp JH, Matthews MA. Int J Hydrogen Energy 1999;24:1123–30.
[27] Shafirovich E, Diakov V, Varma A. Int J Hydrogen Energy 2007;32:207–11.
[28] Hua D, Hanxi Y, Xinping A, Chuansin C. Int J Hydrogen Energy 2003;28:1095–100.
[29] Lu J, Dreisinger DB, Cooper WC. Hydrometallurgy 1997;45:305–22.
[30] Kötz R, Lewerenz HJ, Stucki S. J Electrochem Soc 1983;130:825–9.
[31] Andersson SLT, Howe RF. J Phys Chem 1989;93:4913–20.
[32] Langell MA, Anderson MD, Carson GA, Peng L, Smith S. Phys Rev B 1999;59:4791–8.
[33] Mavel G, Escard J, Costa P, Castaing J. Surf Sci 1973;35:109–16.
[34] Oku M, Hirokawa K. J Electron Spectrosc Relat Phenom 1976;8:475–81.
[35] Wagner CD, Riggs WM, Davis LE, Moulder JF, Mullenberg GE. Handbook of X-ray photoelectron spectroscopy. Eden Prairie, MN 55344: Perkin-Elmer Corporation, Physical Electronics Division; 1979.